

Preliminary Investigation on Plasma Electrolytic Polishing of Microfluidic Platform Produced by Selective Laser Melting

WCMNM
2021

Izidor Sabotin¹, Marko Jerman¹, Andrej Lebar^{1,2}, Joško Valentincič^{1,3}, Toni Böttger⁴, Lisa Kühnel⁴, Henning Zeidler^{4,5}

¹ Faculty of Mechanical Engineering, University of Ljubljana, Aškerčeva 6, SI-1000 Ljubljana, Slovenia

² Faculty of Health Sciences, University of Ljubljana, Slovenia

³ Chair of Microprocess Engineering and Technology - COMPETE, University of Ljubljana, Slovenia

⁴ TU Bergakademie Freiberg, IMKF, Chair of Additive Manufacturing, Agricolastrasse 1, 09599 Freiberg, Germany

⁵ Beckmann-Institut für Technologieentwicklung, Annaberger Strasse 73, 09111 Chemnitz, Germany

Abstract

The inherent issue of additively manufactured metallic parts is in their high surface roughness which hinders technology's applicability for microproduct production. Usually, post-processing is required. Plasma electrolytic Polishing (PeP) is a promising technology which could tackle aforementioned challenges. In this paper, an experimental investigation on improving the quality of metallic microfluidic platforms, printed with selective laser melting (SLM), by applying PeP post-treatment is presented. The results show that overall surface roughness was significantly reduced. Furthermore, the artefacts of SLM technology caused by partial melting and agglomeration of powder at the outside of the melt pool were consistently removed. However, despite the quality improvement due PeP further enhancements of the process chain are necessary to render these microfluidic platforms functional.

Keywords: selective laser melting, plasma electrolytic polishing, process chain, microfluidics, additive technology.

1. Introduction

In the past two decades Additive Manufacturing (AM), popularly denoted as 3D printing, gained significant interest and has been spoken of as a disruptive technology. Since in the process of building the part the material is added, it opens up the possibility to complex part designs which cannot be manufactured by subtractive processes. Nowadays, AM has been successfully utilized in many areas such as aerospace, automotive, electronics, medical and biomedical industries where highly specialized and customizable parts are required [1,2].

Microfluidics is a research field that greatly embraced the AM technologies. With AM truly three-dimensional features can be produced rapidly enabling the research strategy of "fail fast and often". Predominantly polymer based AM technologies are used in microfluidics like inkjet 3D printing, fused deposition modelling, stereolithography and two photon polymerisation.

On the other hand the utilization of metallic materials in microproducts has gained momentum, largely due to its superior properties in view of microproduct performance [3]. Steel microfluidic platforms have several benefits over polymer based such as high robustness, being operational under elevated temperatures and pressures, compatibility with organic solvents and yielding high thermal conductivity coefficients [4].

Among the AM technologies that can print metallic parts direct energy deposition (DED), selective laser sintering (SLS) and selective laser melting (SLM) are the most promising to be utilized in future microfluidic applications [5]. In the view of their implementation SLM has some advantages compared to the former two. SLM exhibits better resolution than DED and it does not need additional processing step, namely sintering, as it is the case with SLS.

SLM is a powder-bed fusion process. A layer of

powder is first spread on the build substrate. In the next step laser beam scans the area related to the particular slice of the part geometry. The exerted heat melts the powder which after solidification joins with the adjacent regions and forms a solid metallic layer. In the next step a new layer of powder is applied to the part surface by a powder-recoating system and the lasers scans the region of the next part geometry slice. The process is repeated until the whole part is built.

An inherent disadvantage of SLM as well as for all metallic AM technologies is the achievable surface quality. Namely, partial melting and/or agglomeration of powder on the surrounding regions of the melt pool leads to high roughness in the range of 10 µm to 30 µm of Ra [6]. For many applications, and especially in microfluidics, these values are inadequate, thus surface finishing is required.

Several postprocessing technologies are currently used to improve surface quality of metallic AM parts. Conventional mechanical technologies such as abrasive flow machining and sandblasting are characterized by low and direction dependent removal rates. Additionally, intense cleaning is required at the end. Established processes such as chemical etching and electro-polishing employ health hazardous concentrated acids or bases. In the last decade laser polishing gained momentum, however the laser spot needs to scan the whole part surface which may be difficult in complex free-form parts. Less common but a promising surface finish technology is plasma electrolytic polishing (PeP) [7].

PeP has gained attention in the metal finishing industry due to its capability to considerably enhance surface properties [8]. PeP is an innovative surface treatment, which renders smooth, high-gloss surfaces with improved corrosion resistance. The process is primarily determined by the dissolution of the anode (the workpiece) and plasma-chemical reactions. In this method a plasma electrolysis takes place in addition to the classical electrolysis. Commonly, the part to be polished is immersed in the electrolyte bath and DC

current is applied between the anode/part and cathode (Fig. 1a). Advantageous aspects of PeP stem from being able to process complex 3D-shaped parts simultaneously over its entire surface and the use of environmentally friendly aqueous electrolytes. The processing temperature at the part surface does not exceed the electrolyte boiling temperature which is below 120 °C.

In this paper a process chain for microfluidic platform consisting of SLM printing and PeP post processing is evaluated through dimensional characterization. Geometrical features of the planar microfluidic platform consist of microchannels and microgrooves, embedded on the microchannel floor, which are commonly applied in bottom groove micromixers.

2. Materials and methods

2.1. SLM 3D printer

For 3D printing of sample microfluidic platforms EOS M 290 SLM printer based on powder-bed fusion was used. It utilises Yb-fibre laser with maximum beam power of 400 W and a laser focus point of 100 µm. Materialise Magics Metal Package and EOSPRINT software was used for CAD/CAM settings.

2.2. SLM printing process parameters

Default process parameters suggested by the CAD/CAM software considering the material and layer depth were applied: laser beam power of 285 W, scanning speed of 960 mm/s, line 'stripes' scanning strategy, hatch spacing of 0.11 mm, powder layer depth of 0.04 mm, N₂ working atmosphere (cca. 0.15% O₂) and the thickness of support layers of 5 mm.

EOS MaragingSteel MS1 powder material was used (X3NiCoMoTi 18-9-5) with a predicted relative density of parts of 8.0 g/cm³.

Three specimens were printed with the same parameters the only difference being the orientation of the parts in *xy*-axis of the powder bed. Specimen 1 was oriented with microfeatures being aligned with the *x*-axis, microfeatures of specimen 2 were parallel to *y*-axis and specimen 3 was tilted for 45° with respect to the specimen 1.

2.3. PeP setup and process parameters

A Pilot plant vat/immersion based PeP machine with a maximum output current of 150 A was used. A stainless-steel vat (max. volume of 200 l) was used as a cathode and a spring clamp was holding the specimen immersed in the electrolyte (Fig. 1b).

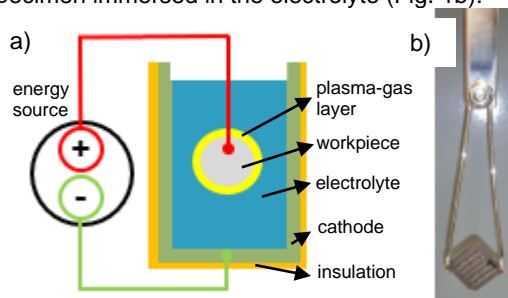


Fig. 1. a) PeP process setup. b) Holder for the specimen.

The previously obtained process parameters for used material to achieve high material removal rate, low surface roughness and high brightness were applied. The used electrolyte was a water solution of ammonium sulphate (0.33 M). The temperature of the electrolyte was kept at 80°C and the specimen was anodically polarized, to sustain the current density of about 0.2 A/cm², with the voltage of 350 V. Treatment times were selected so, that at longest time plateau of roughness reducing curve is reached. The first specimen was treated for 10 min, the second for 15 min and the third for 20 min.

2.4. Microfluidic platform geometry

The design of microfeatures of the microfluidic platform is consistent with the feature shapes that are commonly applied in bottom grooved micromixers. The characteristic grooves at the bottom of the microchannel are either slanted at an angle of 45° with respect to the microchannel (so called slanted grooves - SG) or in a shape of a staggered herringbone (so called herringbone grooves – SH) (Fig. 2).

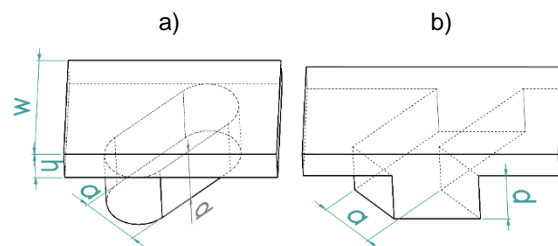


Fig. 2. a) The shape of a SG and b) SH grooves. Geometry denotations: *w* – channel width, *h* – channel height, *a* – groove width, *d* – groove depth.

The optimal aspect ratios of grooves (*d/a*) are a function of the microchannel aspect ratio (*h/w*) and were determined from research papers [9,10]. One should note that the optimal aspect ratio of a SH groove is smaller compared to optimal SG groove.

Three sizes (L, M, S) of sample micromixer geometries were incorporated in the specimen design (Fig. 3). The dimensions of geometries are gathered in Table 1. Depths of features were set so, that they correspond to a multiplier of a single layer powder depth of 40 µm.

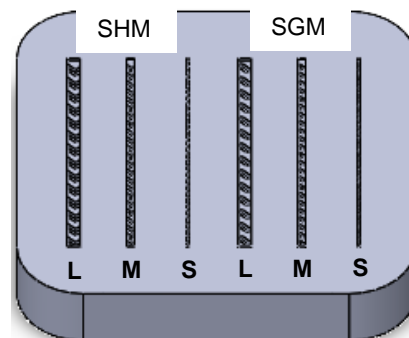


Fig. 3. 3D model of a microfluidic specimen (30x30x3 mm) with denotations: SHM – staggered herringbone micromixer design, SGM – slanted groove micromixer design.

Samples of groove micromixer geometries were modelled as parallel microchannels with descending sizes from large (L) to small (S).

2.5. Measurements

Characterisation measurements were conducted on a Keyence VHX-6000 digital microscope. The 3D surface was acquired using depth composition function. Profile roughness (R_a) was determined by MarSurf PS 10 profilometer.

Table 1. Nominal dimensions of micromixer designs

Variant	Feature			
	w [μm]	h [μm]	a [μm]	d [μm]
SGM-L	1000	280	500	480
SGM-M	600	160	300	320
SGM-S	200	80	100	80
SHM-L	1000	280	500	400
SHM-M	600	160	300	240
SHM-S	200	80	100	80

3. Results and discussion

3.1. SLM printed specimens

The first observation of printed microfluidic platforms is, that different orientation of the parts on the machine xy table did not result in different print quality. This is due to the fact, that the laser trajectory at microfeature edges follows the edge contour, thus bulk hatch orientation influences only larger surfaces not crucial for microfeature geometries. Correspondingly, all the edges of microfeatures have a ridge of approximate height of $\sim 10 \mu\text{m}$.

As expected, larger (L) micromixer designs are printed with better geometrical quality (Fig. 4a,d). However, solidified microspheres with the diameter of used metal dust can be observed on the side walls of the microchannel and in the grooves (Fig. 6a). Middle (M) sized designs are printed with bigger defects. In the grooves often a micropillar is present, which is a consequence of agglomerated resolidified dust particles (Fig. 6a). The explanation of mentioned artefacts lies in presence of dust particles near the edges of microfeatures which should not be melted by laser beam, however, they are melted due to excess heat. For the smallest designs (S) the microgrooves are below the printer's resolution (e.g. diameter of laser focus point is $100 \mu\text{m}$) thus, they are printed into shapes that hardly correspond to a groove (Fig. 4c,f). Corresponding microchannels are printed more reliably with high relative width deviation.

The surface roughness was measured in the middle part of the specimens. The R_a values for specimens 1, 2 and 3 were $18.5 \pm 0.4 \mu\text{m}$, $18.2 \pm 0.5 \mu\text{m}$ and $18.6 \pm 0.3 \mu\text{m}$ respectively which is in a typical range for SLM printed parts. This roughness exceeds the values for typical microfluidic applications ($R_a < 1 \mu\text{m}$) by a lot, thus specimens were subjected to PeP treatment to reduce it.

3.2. Specimens after PeP treatment

At larger micromixer designs even after the shortest PeP treatment (specimen 1) significant improvement of the microfeatures quality is observed. Formed microspheres at the groove edges and on the bottom of the grooves were removed (Fig. 5). This is because higher electric field is present at pointy

artefacts thus the PeP process removes them. Also, the waviness due to the laser scanning hatch pattern got severely reduced (Fig. 7). Similar observations can be made with regards to medium sized microfeatures. Furthermore, the occasional micropillars within the grooves were also removed by the PeP as is evident from Fig. 6.

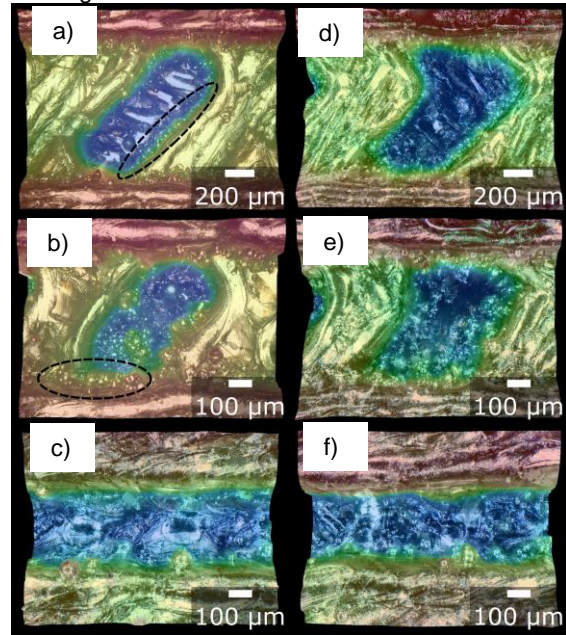


Fig. 4. Microscope images of single grooves (specimen 1). a) SG-L, dashed ellipse highlights solidified spheres, b) SG-M, solidified spheres at the channel edge are highlighted, c) SG-S, d) SH-L, e) SH-M and f) SH-S.

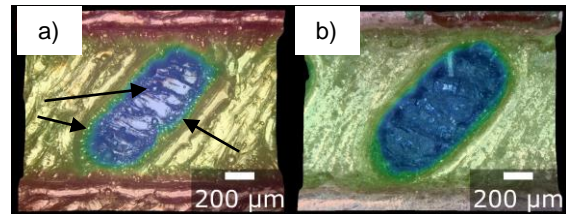


Fig. 5. Pre (left) and post (right) PeP treated specimen 1 detail (SG-L). The arrows point to solidified microspheres.

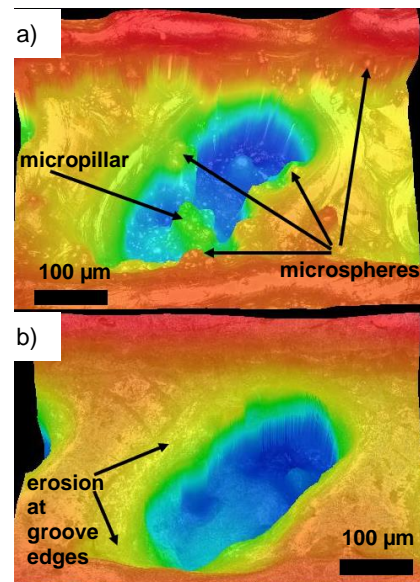


Fig. 6. A colored height microscopic image of a specimen 1 SG-M groove a) before and b) after PeP treatment.

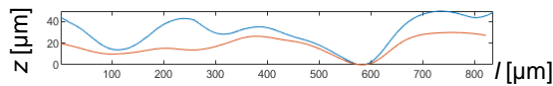


Fig. 7. Bottom profile at the middle of a SG-L groove before (blue line) and after (red line) PeP treatment.

However, a damaging effect of PeP can be observed on groove edges where additional material removal occurred (Fig. 6b).

The influence of the PeP treatment duration can be extrapolated from Fig. 8. After shortest treatment time (10 min, Fig. 5b) the effects are consistent with above observations, namely, the microspheres and possible micropillars were eroded.

Longer PeP treatment (15 min, Fig. 8a) resulted in significant material removal also at the main channel side walls. 20 min PeP treatment (Fig. 8b) resulted in greater deterioration at the microchannel side walls. Furthermore, microcracks appeared at the groove edges and bottom.

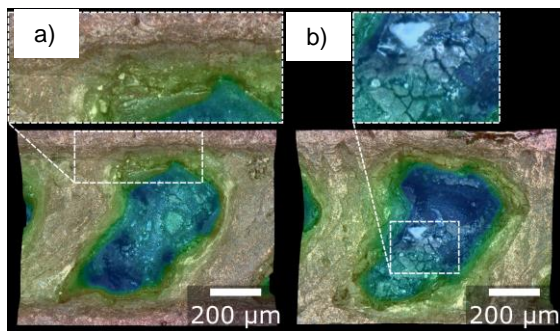


Fig. 8. SH-M grooves after PeP treatment. a) PeP treatment for 15 min (specimen 2) where erosion at the channel edge is highlighted. b) PeP treatment for 20 min (specimen 3) where microcracks at the bottom of the groove are seen.

The roughness on the flat surfaces of specimens was significantly reduced. Similar R_a values were measured on all three specimens regardless of the PeP treatment duration. For specimen 1 average roughness value was $2.7 \pm 0.3 \mu\text{m}$, for specimen 2 $2.8 \pm 0.3 \mu\text{m}$ and specimen 3 $2.5 \pm 0.3 \mu\text{m}$. This means that the shortest PeP treatment was the best option since low frequency waviness of the pre-treated parts is harder to remove. However, the roughness still exceeds the values acceptable in microfluidics.

4. Conclusions

In this paper, the influence of PeP treatment of SLM printed microfluidic platforms is presented. The results show that PeP treatment significantly improves microfeatures quality by removing resolidified microspheres at the feature edges and reduces overall roughness. Even the occasional occurrence of micropillar artefacts in the medium sized grooves were removed. Three durations of PeP were tested and the shortest treatment has proved to be the best. At longer PeP times, the edges of the microfeatures got eroded and there is a possibility of material surface microcracking.

This brief investigation shows that PeP is a promising post-treatment technology which can improve the SLM printed microfluidic platforms quality. However, the drawback of higher erosion at sharp edges of microfeatures should be thoroughly investigated in the future.

Acknowledgements

This work was supported by the Slovenian Research Agency (ARRS) (Grant No. P2-0248 (B)) and EU EC H2020 funded Era Chair of Micro Process Engineering and Technology – COMPETE (Grant No. 811040). Authors wish to thank Boštjan Podlipec and SiEVA ltd. for providing resources for SLM printing.

References

- [1] Waheed, S., Cabot, J. M., Macdonald, N. P., Lewis, T., Guijt, R. M., Paull, B., and Breadmore, M. C., 2016, "3D Printed Microfluidic Devices: Enablers and Barriers," *Lab Chip*, **16**(11), pp. 1993–2013.
- [2] Guo, N., and Leu, M. C., 2013, "Additive Manufacturing: Technology, Applications and Research Needs," *Front. Mech. Eng.*, **8**(3), pp. 215–243.
- [3] Alting, L., Kimura, F., Hansen, H. N., and Bissacco, G., 2003, "Micro Engineering," *CIRP Ann. - Manuf. Technol.*, **52**(2), pp. 635–657.
- [4] Gjuraj, E., Kongoli, R., and Shore, G., 2012, "Combination of Flow Reactors with Microwave-Assisted Synthesis: Smart Engineering Concept for Steering Synthetic Chemistry on the 'Fast Lane,'" *Chem. Biochem. Eng. Q.*, **26**(3), pp. 285–307.
- [5] Nagarajan, B., Hu, Z., Song, X., Zhai, W., and Wei, J., 2019, "Development of Micro Selective Laser Melting: The State of the Art and Future Perspectives," *Engineering*, **5**(4), pp. 702–720.
- [6] Zeidler, H., Böttger-Hiller, F., Krinke, S., Parenti, P., and Annoni, M., 2019, "Surface Finish of Additively Manufactured Parts Using Plasma Electrolytic Polishing," *19th International Conference and Exhibition, EUSPEN 2019*, pp. 228–229.
- [7] Zeidler, H., and Böttger-Hiller, F., 2018, "Surface Finish of Additively Manufactured Parts Using Plasma Electrolytic Polishing | Request PDF," *WCMNM 2018*, J. Valentinčič, M.B.-G. Jun, K. Dohda, and S.S. Dimov, eds., Research Publishing, Singapore, Portorose, Slovenia.
- [8] Parfenov, E. V., Yerokhin, A., Nevyantseva, R. R., Gorbakov, M. V., Liang, C. J., and Matthews, A., 2015, "Towards Smart Electrolytic Plasma Technologies: An Overview of Methodological Approaches to Process Modelling," *Surf. Coatings Technol.*, **269**(1), pp. 2–22.
- [9] Sabotin, I., Tristo, G., Junkar, M., and Valentinčič, J., 2013, "Two-Step Design Protocol for Patterned Groove Micromixers," *Chem. Eng. Res. Des.*, **91**(5).
- [10] Lynn, N. S., and Dandy, D. S., 2007, "Geometrical Optimization of Helical Flow in Grooved Micromixers," *Lab Chip*, **7**(5), pp. 580–587.